# Effect of Excited-State Structural Relaxation on Midgap Excitations in Co2+-Doped ZnO Quantum Dots

**ARTICLE** *in* THE JOURNAL OF PHYSICAL CHEMISTRY C · JUNE 2014

Impact Factor: 4.77 · DOI: 10.1021/jp501360d



**4 AUTHORS**, INCLUDING:

Joseph May
University of Washington Seattle
**9** PUBLICATIONS **33** CITATIONS

SEE PROFILE

Ekaterina Badaeva
The Boeing Company
**26** PUBLICATIONS **724** CITATIONS

SEE PROFILE

THE JOURNAL OF PHYSICAL CHEMISTRY C

Article

pubs.acs.org/JPCC

# Effect of Excited-State Structural Relaxation on Midgap Excitations in $Co^{2+}$-Doped ZnO Quantum Dots

Joseph W. May, Jiao Ma, Ekaterina Badaeva, and Xiaosong Li*

Department of Chemistry, University of Washington, Seattle, Washington 98195, United States

**ABSTRACT:** The unique midgap excited states of $Co^{2+}$-doped ZnO quantum dots have given rise to new applications in photocatalysis, sensing, magneto-optics, and magnetoelectronics. However, the electronic characteristics of these midgap transitions are not fully understood, and the uncertain interplay between these transitions has led to disagreement in the literature. In this work, midgap excited states of $Co^{2+}$-doped ZnO quantum dots are analyzed using linear response time-dependent density functional theory and the effective mass theory with a focus on the geometry relaxation in the donor-type photoionization excited state. Relaxation of the excited-state geometry lowers the charge-transfer transition energy to be in the vicinity of the prominent spin-allowed $^4A_2 \rightarrow {}^4T_1$ $Co^{2+}$ d−d transition that gives this material its characteristic color. For large quantum dots, the excited-state population distribution between this $Co^{2+}$ d−d excited state and the charge-transfer excited state can be tuned by thermal energy, resulting in a unique temperature dependence of the luminescence and photoconductivity.

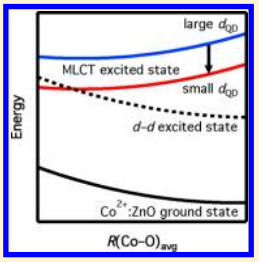


## INTRODUCTION

Semiconducting materials doped with transition-metal ions have attracted broad interest due to their applications in photocatalysis, photovoltaics, and spin electronics.[1−10] For $Co^{2+}$-doped ZnO ($Co^{2+}$:ZnO), these applications are strongly influenced by the material's complex electronic structure, which derives from the fact that the $Co^{2+}$ 3d levels are located within the band gap of the ZnO semiconductor host. This feature gives rise to new spectral bands in the visible energy region, including ligand-field (d−d) transitions centered at the dopant and charge-transfer (CT) bands. These CT bands, frequently referred to as donor- and acceptor-type photoionization transitions, involve the promotion of a localized $Co^{2+}$ d electron into a delocalized conduction band (CB) orbital, referred to as metal-to-ligand charge transfer ($ML_{CB}CT$), or promotion of a valence band (VB) electron into a localized $Co^{2+}$ d orbital, referred to here as a ligand-to-metal charge transfer ($L_{VB}MCT$) transition.[11] However, the electronic characteristics of these midgap transitions are not fully understood, and the uncertain assignment of the energies of these transitions in $Co^{2+}$:ZnO has led to disagreement in the literature.

The electronic structure of $Co^{2+}$-doped ZnO has been investigated extensively at both the fundamental level and in relation to potential spin-based electronics applications.[12−15] Despite extensive research, the characteristics and interplay of its dopant-centered midgap electronic excited states remain unclear. Kanai and co-workers first reported room-temperature midgap photoconductivity in $Co^{2+}$:ZnO following $Co^{2+}$ d−d excitation to the broad and structured $^4A_2 \rightarrow {}^4T_1(P)$ band centered at ∼2.0 eV.[16] From this observation, it was concluded that the $Co^{2+}$ $^4T_1(P)$ manifold must reside "near or in the CB of ZnO" so that the photoexcited $Co^{2+}$ d electron can relax to the $ML_{CB}CT$ band and give rise to the observed photocurrent. This observation is not easily reconciled with subsequent observations of photoluminescence from the same d−d band,[17,18] which might suggest instead that the $Co^{2+}$ $^4A_2 \rightarrow {}^4T_1(P)$ d−d transition lies below the $ML_{CB}CT$ threshold.[18] Recent studies of $Co^{2+}$:ZnO epitaxial films have identified the source of this discrepancy by showing a strong dependence of d−d photoconductivity on both temperature and $Co^{2+}$ concentration, leading to a picture in which the $^4T_1(P)$ excited state is slightly above the $ML_{CB}CT$ state at low $Co^{2+}$ concentrations (∼0.8%) but below the $ML_{CB}CT$ state at higher concentrations (∼11%), allowing the former to show d−d photoconductivity but not the latter.[19,20] For all concentrations, the d−d photoconductivity is thermally activated, with an activation barrier for electron ionization to the ZnO CB that depends on the $Co^{2+}$ concentration. These results illustrate the complexity of the electronic structure of this experimentally well-studied material.

A number of theoretical efforts have been carried out to understand the electronic structure of $Co^{2+}$:ZnO as well, including the energies and characteristics of its midgap excited states.[21−24] Excitations in condensed matter are often approximated as the difference in orbital energies for the occupied and unoccupied (or virtual) orbitals obtained from ground-state density functional theory (DFT) calculations.[22,25] This method gives reasonable results for systems with moderate correlation and small electron−hole binding energies. Linear response time-dependent density functional theory (TDDFT) provides a more accurate assessment of excited-state energies and wave functions, and TDDFT has been applied recently to describe the excited-state electronic structures of $Co^{2+}$:ZnO quantum dots (QDs).[11,26] These TDDFT studies predict the $Co^{2+}$ d−d excitation to be located below the $ML_{CB}CT$ band in these QDs but neglect the important role played by nuclear

**Received:** February 7, 2014
**Revised:** May 26, 2014
**Published:** May 27, 2014

   dx.doi.org/10.1021/jp501360d | J. Phys. Chem. C 2014, 118, 13152−13156

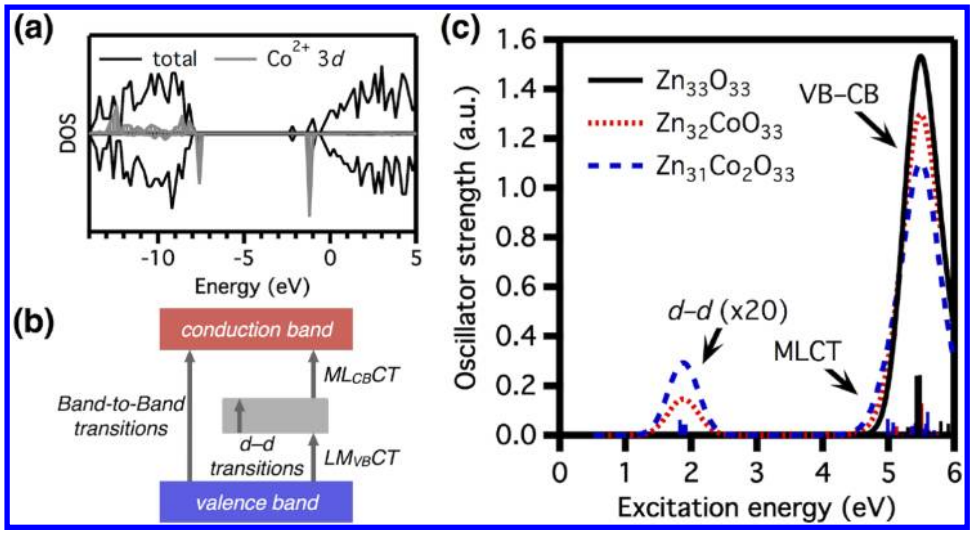


**Figure 1.** (a) DOS diagram calculated for a $CoZn_{32}O_{33}$ QD. The shaded region shows the $Co^{2+}$ 3d contribution to the DOS diagram magnified by 5×. Spin-up, positive density values; spin-down, negative density values. (b) Schematic illustration of the optical transitions observed in $Co^{2+}$:ZnO. Note that, experimentally, the $L_{VB}$MCT and $ML_{CB}$CT transition energies do not sum to the band-to-band transition energy as they are depicted because of large electron−electron repulsion effects at the $Co^{2+}$ dopant. (c) TDDFT absorption spectra of a pure $Zn_{33}O_{33}$ QD (solid black curve), a $Zn_{32}CoO_{33}$ QD with one $Co^{2+}$ dopant (dotted red curve), and a $Zn_{31}Co_2O_{33}$ QD with two $Co^{2+}$ dopants (dashed blue curve). The $^4A_2 \rightarrow {}^4T_1(P)$ bands at ∼2 eV are magnified 20-fold. The line shape functions were obtained by fitting the calculated spectral lines with Gaussian functions having a line broadening parameter of 0.16 eV.

relaxation upon electronic excitation. Addressing the role of structural relaxation on the excited state may provide a better understanding of the midgap transitions and, hence, the physical properties of this important material.

In this work, we present a theoretical analysis of the excited-state structural relaxation pathways, energy levels, and mechanisms governing the photoconductivity and luminescence in $Co^{2+}$:ZnO QDs following ligand-field excitations. The results account for the explicit role of nuclear relaxation in the d−d and $ML_{CB}$CT excited states.

## METHODOLOGY

All calculations were performed with the development version of the Gaussian program.[27] Nanocrystal electronic structures were obtained with the PBE1PBE hybrid DFT functional.[28−30] The Los Alamos double-ζ pseudocore potential (LANL2DZ)[31−33] and the associated basis set were used for the ZnO lattice with the Zn (4s, 3d) and O (1s, 2s, 2p) atomic orbitals treated with explicit basis functions. Cobalt dopants were modeled with the Los Alamos valence triple-ζ pseudocore potential (LANL2TZ) and basis set.[34] The electronic excited-state energies and wave functions of $Co^{2+}$:ZnO QDs were calculated using TDDFT within the linear response framework. Absorption spectra were obtained by dressing the excited-state peaks resulting from the TDDFT calculation with Gaussian functions having a broadening constant of 0.16 eV to best fit the experimental data. Nearly spherical wurtzite ZnO nanocrystals, $Zn_{21}O_{21}$ (diameter ≈ 0.7 nm), $Zn_{33}O_{33}$ (diameter ≈ 1.2 nm), and $Zn_{84}O_{84}$ (diameter ≈ 2.0 nm) were constructed according to the previously published scheme.[11,26] The dangling bonds on the surface of the nanocrystals were passivated with pseudohydrogen atoms having modified nuclear charges of 0.5 and 1.5 to terminate surface $O^{2-}$ and $Zn^{2+}$ ions, respectively. Excited-state geometry optimizations were performed within the TD-PBE1PBE/LANL2DZ level of theory, following the excited-state gradients.

## RESULTS AND DISCUSSION

Figure 1a shows the density of states (DOS) diagram calculated for a $Zn_{32}CoO_{33}$ QD showing a filled VB and empty CB separated by a gap of $E_g \approx 5.8$ eV, larger than the bulk band gap of ∼3.4 eV due to quantum confinement. Also shown in the DOS diagram is the contribution of the $Co^{2+}$ 3d electrons. In the pseudotetrahedral crystal field of wurtzite ZnO, the $Co^{2+}$ 3d electrons with the same spin are split by symmetry into two lower-energy $d_e$ and three higher-energy $d_{t_2}$ orbitals, whereas exchange interactions lead to the splitting between electrons with different spins. The ground state of $Co^{2+}$ is a high-spin $d^7$ ($S = 3/2$) configuration. Whereas, all of the $Co^{2+}$ spin-up 3d levels are covalently delocalized into the VB of the semiconductor, the spin-down electrons are much more localized, appearing ∼1 eV above the edge of the ZnO VB. These results agree well with experimental photoemission data.[35−37]

The new states introduced into the ZnO band gap by the $Co^{2+}$ dopant give rise to new, lower-energy excitations, as seen in the absorption spectra in Figure 1c. These new transitions are characterized in the schematic in Figure 1b and have been previously well characterized.[11,19] Figure 1c shows the absorption spectrum for a $Zn_{32}CoO_{33}$ QD (3% $Co^{2+}$:ZnO) and a $Zn_{31}Co_2O_{33}$ QD (6% $Co^{2+}$:ZnO) of 1.2 nm diameter calculated with the linear response TDDFT approach,[38] compared to that of a pure $Zn_{33}O_{33}$ QD. The two lowest-energy absorption bands (at ∼0.8 and ∼1.85 eV) correspond to the $Co^{2+}$ $^4A_2 \rightarrow {}^4T_1(F)$ and $^4A_2 \rightarrow {}^4T_1(P)$ ligand-field transitions, respectively. These transitions have nonzero oscillator strengths as a result of hybridization (covalency) with the ZnO lattice. The excitation energies are essentially independent of QD diameter, whereas the oscillator strengths are dependent on the dopant concentration. The shoulder in the higher midgap energy region (starting at ∼4.1 eV) results from the $ML_{CB}$CT transitions, which split into two sub-bands, MLCT1 and MLCT2. These two sub-$ML_{CB}$CT bands correspond to excitations of $Co^{2+}$ $d_e$ and $d_{t_2}$ electrons to the


dx.doi.org/10.1021/jp501360d | J. Phys. Chem. C 2014, 118, 13152−13156

ZnO CB, respectively. For detailed characteristics of these transitions, we refer readers to our previous theoretical work on the absorption spectra of doped ZnO QDs.[11,39] For the $Zn_{32}CoO_{33}$ QD of 1.2 nm diameter, the highest d−d and the lowest $ML_{CB}CT$ vertical excitations are separated by ∼2.3 eV. This amount of energy cannot be compensated for by room-temperature thermal activation. As a result, theoretical predictions of the vertical excitations of smaller QDs cannot explain the photoconductivity following excitation to the $^4T_1$ d−d excited state.

As the QD diameter increases, the energetic separation between the $Co^{2+}$ d−d and $ML_{CB}CT$ bands will change, possibly leading to an energetic crossover. The $Co^{2+}$ d−d excitation is localized and independent of QD diameter. The $ML_{CB}CT$ band intrinsically depends on the CB levels, which decrease in energy with increasing QD diameter due to quantum confinement. As a result, the energetic separation between the $Co^{2+}$ d−d and $ML_{CB}CT$ bands will decrease as the QD diameter increases. This phenomenon can be understood using the effective mass approximation for a spherical QD.[11,40] In the absorption spectrum, energy shifts of the $ML_{CB}CT$ band, $\Delta E_{MLCT}$, and the band-to-band excitonic transition, $\Delta E_{EXC}$, compared to those in bulk ZnO, take on the approximate relationship

$$\frac{\Delta E_{MLCT}}{\Delta E_{EXC}} \approx \frac{m_e^{*-1}}{m_e^{*-1} + m_h^{*-1}} \quad (1)$$

where $m_e^*$ and $m_e^*$ are the effective masses (in units of electron mass) of the electron and hole in $Co^{2+}$:ZnO. The effective mass of the electron has been approximated to be 0.59 and 0.72 for MLCT1 and MLCT2, respectively, in $Co^{2+}$:ZnO.[11]

Equation 1 can be used to extrapolate the energy of the $ML_{CB}CT$ band to the bulk limit. Figure 2 shows the extrapolation using eq 1 of the MLCT1 absorption transition to the bulk band gap limit of 3.4 eV for ZnO. The validity of eq 1 is confirmed by calculations on QDs with different diameters. In the same figure, the d−d absorption is also plotted. This transition energy appears fixed, independent of QD diameter, consistent with its highly localized orbital nature. At the bulk band gap limit of 3.4 eV, the MLCT1 excitations still occur much higher in energy than the d−d transitions, almost 40 times $k_BT$ at room temperature without structural relaxation. By taking into account the nuclear relaxation of the excited state, the energy difference between the $ML_{CB}CT$ and $^4T_1$ d−d bands is still 10 times $k_BT$ at room temperature. An energy level scheme like this would be consistent with photoluminescence from the d−d excited state back to the ground state, while ruling out the possibility of photoconductivity. Experimentally, however, photoconductivity was observed in 4% $Co^{2+}$:ZnO epitaxial films following $^4A_2 \rightarrow {}^4T_1(P)$ excitation even at 27 K.[19] This observation implies that a relaxation pathway must exist for the d−d excited-state population to be transferred to the $ML_{CB}CT$ excited state.

We hypothesize that a $ML_{CB}CT$ relaxation pathway could possibly arise from electron−nuclear coupling, which causes geometry relaxation on the excited-state potential energy surface (PES). Such a relaxation pathway will make vertical absorption transition energies different from the equilibrium excited-state energies relevant to the population thermalization of the experimental observations. To test this hypothesis, the excited-state structures were fully optimized at the TD-PBE1PBE level of theory. Figure 3 shows the changes in the

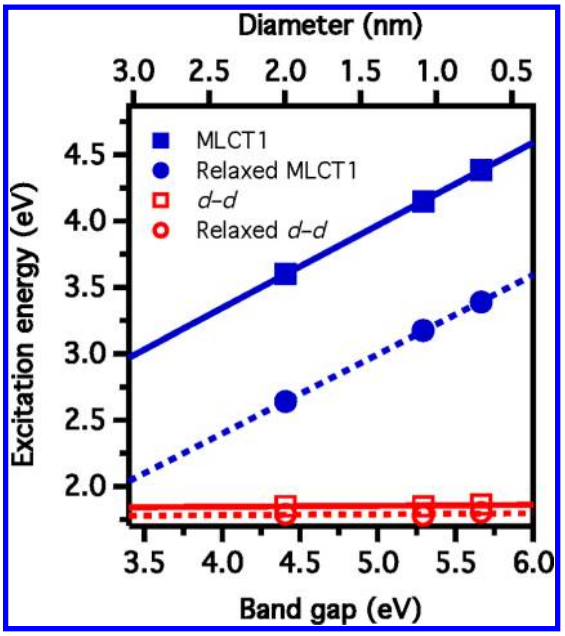


**Figure 2.** Calculated MLCT1 (■,●) and $Co^{2+}$ d−d (□,○) transition energies for $Co^{2+}$:ZnO QDs of decreasing diameter (2.0, 1.2, and 0.7 nm from left to right), plotted against the first excitonic transition energy and extrapolated to the bulk band gap limit of 3.4 eV. For the MLCT1 and d−d transitions, the excitation energies at the ground-state geometry (solid lines) and at the optimized excited-state geometry (dashed lines) are included.

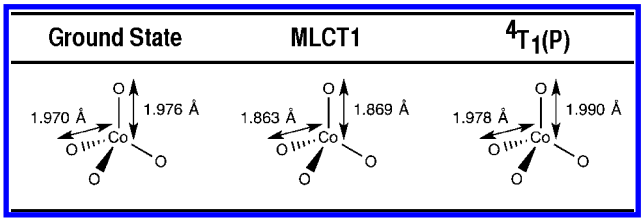


**Figure 3.** A comparison of the MLCT and $Co^{2+}$ d−d excited-state geometries for a $Zn_{32}CoO_{33}$ QD before and after relaxation of the lattice to the respective excited-state minimum.

excited-state geometries after the lattice relaxes to minimize the excited-state energy. The MLCT1 transitions formally promote an electron from $Co^{2+}$ to the CB of ZnO, resulting in a charge state approaching $Co^{3+}$ ($d_{t_2}^2$ configuration), and should induce a contraction of the Co−O bonds in this excited state. Our TDDFT results show that all Co−O bonds shorten by ∼0.1 Å in this MLCT1 excited state relative to the ground state, lowering the overall MLCT1 energy by ∼1 eV. By comparison, the nuclear relaxation in the d−d excited state is much smaller, corresponding to substantially less energy stabilization (∼0.05 eV in the 1.2 nm QD). For the small QDs considered here (diameter = 0.7, 1.2, and 2.0 nm), the fully relaxed minima of the MLCT1 and d−d excited states are still energetically well separated, attributed to the large quantum confinement energies in these very small nanocrystals. From eq 1, relaxation of this quantum confinement by increasing the QD diameter to approach the bulk limit will shift the MLCT1 excited state downward toward the d−d excited state. As shown in Figure 2, the MLCT1 electronic energies in their fully optimized excited-state geometries follow the prediction of the effective mass theory in eq 1, whereas the d−d excited-state energies are fixed, independent of quantum confinement. The MLCT1 electronic


dx.doi.org/10.1021/jp501360d | J. Phys. Chem. C 2014, 118, 13152−13156

origin is predicted to red shift to ~2.0 eV at the bulk band gap limit of 3.4 eV, slightly higher (~0.15 eV) in energy than the vertical d−d transitions and in generally good agreement with the energy of ~0.1 eV estimated from experiment.[19,20]

The energies presented above relate to relaxation of the d−d and $ML_{CB}CT$ excited states along their independent nuclear reorganization coordinates, which are shown schematically in Figure 3. Thermally activated transitions between these two excited states, as seen experimentally,[19,20] arise from local lattice vibrations that connect these two geometries. Figure 4 shows

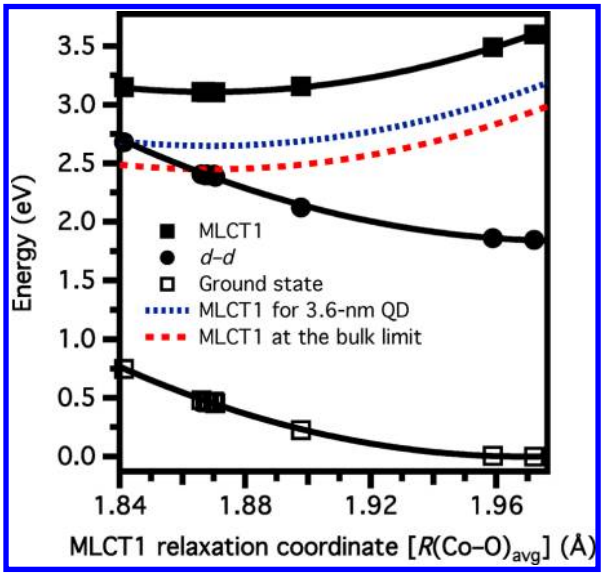


**Figure 4.** PESs of the ground, d−d, and MLCT1 excited states for a $Zn_{83}CoO_{84}$ QD (diameter ≈ 2.0 nm) plotted along the effective MLCT1 nuclear reorganization coordinate, represented here as $R(Co-O)_{avg}$.

the d−d and MLCT1 excited-state PESs of the ~2.0 nm QD ($Zn_{84}O_{84}$) plotted along the MLCT1 nuclear relaxation coordinate, represented by the average Co−O bond length, $R(Co-O)_{avg}$. In the equilibrium geometry of the ground state, $R(Co-O)$ = 1.972 Å. In the relaxed d−d excited state, $R(Co-O)$ shows a ~0.01 Å deviation from the ground-state bond length. In the relaxed MLCT1 state, however, $R(Co-O)$ contracts to 1.86−1.87 Å and results in a nuclear reorganization energy of ~0.5 eV. This large nuclear reorganization is responsible for the broad spectral distribution of the $ML_{CB}CT$ transition intensities observed experimentally.[19,20] Figure 4 also plots the MLCT1 PESs estimated for different degrees of quantum confinement using the effective mass approximation of eq 1. In the bulk limit, the MLCT1 PES crosses that of the $^4T_1(P)$ d−d excited state. Thermal population of this MLCT1 PES will favor charge separation and reduce d−d luminescence. Equation 2 describes the relationship between the shift in the $ML_{CB}CT$ energy and the photoexcited electron's effective mass[11]

$$\Delta E_{MLCT} \approx \frac{\hbar^2\pi^2}{2r^2}\left[\frac{1}{m_e^*}\right] - \frac{1.8e^2}{\epsilon r} \quad (2)$$

where the Coulomb interaction between the photogenerated CB electron and localized hole has been neglected. Using an effective mass of $m_e^*$ = 0.59 in eq 2, we compute a critical QD diameter of ~3.6 nm at which the $ML_{CB}CT$ PES will cross the $Co^{2+}$ $^4T_1(P)$ PES at the $ML_{CB}CT$ equilibrium geometry.

## CONCLUSION

Figure 4 is helpful for interpreting the experimental observations related to photoconductivity and luminescence quenching in $Co^{2+}$:ZnO. In small QDs, quantum confinement leads to higher-energy $ML_{CB}CT$ excited states that are not thermally accessible from the $^4T_1(P)$ state. In large QDs and bulk $Co^{2+}$:ZnO, these states are shifted closer to the d−d excited state. In all cases, excited-state nuclear relaxation stabilizes the $ML_{CB}CT$ excited state by ~0.5 eV, bringing it much closer to the d−d excited-state energy. Photoluminescence from the $^4T_1(P)$ state thus becomes more favorable with increasing quantum confinement and lower temperature, whereas d−d photoconductivity shows the opposite trends. These computational results complement recent experimental interpretations and furthermore provide new insights into possible mechanisms for tuning the interplay between the delocalized $ML_{CB}CT$ photoionization excited states and the localized ligand-field excited states of $Co^{2+}$:ZnO, which may be of interest for photocatalytic reactions or other photoinduced charge separation applications.

## AUTHOR INFORMATION

### Corresponding Author

*E-mail: li@chem.washington.edu.

### Notes

The authors declare no competing financial interest.

## ACKNOWLEDGMENTS

This work was supported by the U.S. National Science Foundation (CHE-1265945) and the Department of Energy (DE-SC0006863). Additional support of the University of Washington Student Technology Fund and the Royalty Research Fund is gratefully acknowledged.

## REFERENCES

(1) Zou, Z.; Ye, J.; Sayama, K.; Arakawa, H. Direct Splitting of Water under Visible Light Irradiation with an Oxide Semiconductor Photocatalyst. *Nature* **2001**, *414*, 625−627.

(2) Osterloh, F. E. Inorganic Materials as Catalysts for Photochemical Splitting of Water. *Chem. Mater.* **2008**, *20*, 35−54.

(3) Kramer, I. J.; Sargent, E. H. Colloidal Quantum Dot Photovoltaics: A Path Forward. *ACS Nano* **2011**, *5*, 8506−8514.

(4) Ip, A. H.; Thon, S. M.; Hoogland, S.; Voznyy, O.; Zhitomirsky, D.; Debnath, R.; Levina, L.; Rollny, L. R.; Carey, G. H.; Fischer, A.; et al. Hybrid Passivated Colloidal Quantum Dot Solids. *Nat. Nanotechnol.* **2012**, *7*, 577−582.

(5) Kamat, P. V. Quantum Dot Solar Cells. The Next Big Thing in Photovoltaics. *J. Phys. Chem. Lett.* **2013**, *4*, 908−918.

(6) Zhu, H.; Song, N.; Lian, T. Charging of Quantum Dots by Sulfide Redox Electrolytes Reduces Electron Injection Efficiency in Quantum Dot Sensitized Solar Cells. *J. Am. Chem. Soc.* **2013**, *135*, 11461−11464.

(7) Wolf, S. A.; Awschalom, D. D.; Buhrman, R. A.; Daughton, J. M.; von Molnár, S.; Roukes, M. L.; Chtchelkanova, A. Y.; Treger, D. M. Spintronics: A Spin-Based Electronics Vision for the Future. *Science* **2001**, *294*, 1488−1495.

(8) Loss, D.; DiVincenzo, D. P. Quantum Computation with Quantum Dots. *Phys. Rev. A* **1998**, *57*, 120−126.

(9) Žutić, I.; Fabian, J.; Sarma, S. D. Spintronics: Fundamentals and Applications. *Rev. Mod. Phys.* **2004**, *76*, 323−410.

(10) Awschalom, D. D.; Bassett, L. C.; Dzurak, A. S.; Hu, E. L.; Petta, J. R. Quantum Spintronics: Engineering and Manipulating Atom-Like Spins in Semiconductors. *Science* **2013**, *339*, 1174−1179.

(11) Badaeva, E.; Isborn, C. M.; Feng, Y.; Ochsenbein, S. T.; Gamelin, D. R.; Li, X. Theoretical Characterization of Electronic

Transitions in $Co^{2+}$- and $Mn^{2+}$-Doped ZnO Nanocrystals. *J. Phys. Chem. C* **2009**, *113*, 8710−8717.
(12) Song, C.; Geng, K. W.; Zeng, F.; Wang, X. B.; Shen, Y. X.; Pan, F.; Xie, Y. N.; Liu, T.; Zhou, H. T.; Fan, Z. Giant Magnetic Moment in an Anomalous Ferromagnetic Insulator: Co-Doped ZnO. *Phys. Rev. B* **2006**, *73*, 024405.
(13) Yao, T.; Yan, W.; Sun, Z.; Pan, Z.; Xie, Y.; Jiang, Y.; Ye, J.; Hu, F.; Wei, S. Magnetic Property and Spatial Occupation of Co Dopants in $Zn_{0.98}Co_{0.02}O$ Nanowires. *J. Phys. Chem. C* **2009**, *113*, 14114−14118.
(14) Xu, M.; Zhao, H.; Ostrikov, K.; Duan, M. Y.; Xu, L. X. Effect of Doping with Co and/or Cu on Electronic Structure and Optical Properties of ZnO. *J. Appl. Phys.* **2009**, *105*, 043708.
(15) Azam, A. Fabrication of Co-Doped ZnO Nanorods for Spintronic Devices. *Met. Mater. Int.* **2013**, *19*, 845−850.
(16) Kanai, Y. Optical Absorption and Conduction Due to $Co^{2+}$ in ZnO Crystals. *J. Phys. Soc. Jpn.* **1968**, *24*, 956.
(17) Lommens, P.; Smet, P. F.; de Mello Donegá, C.; Meijerink, A.; Piraux, L.; Michotte, S.; Mátéfi-Tempfli, S.; Poelman, D.; Hens, Z. Photoluminescence Properties of $Co^{2+}$-Doped ZnO Nanocrystals. *J. Lumin.* **2006**, *118*, 245−250.
(18) Schultz, H.-J.; Thiede, M. Optical Spectroscopy of $3d^7$ and $3d^8$ Impurity Configurations in a Wide-Gap Semiconductor (ZnO:Co, Ni, Cu). *Phys. Rev. B* **1987**, *35*, 18−34.
(19) Johnson, C. A.; Kaspar, T. C.; Chambers, S. A.; Salley, G. M.; Gamelin, D. R. Sub-Band-Gap Photoconductivity in $Co^{2+}$-Doped ZnO. *Phys. Rev. B* **2010**, *81*, 125206.
(20) Johnson, C. A.; Cohn, A.; Kaspar, T.; Chambers, S. A.; Salley, G. M.; Gamelin, D. R. Visible-Light Photoconductivity of $Zn_{1-x}Co_xO$ and Its Dependence on $Co^{2+}$ Concentration. *Phys. Rev. B* **2011**, *84*, 125203.
(21) Koidl, P. Optical Absorption of $Co^{2+}$ in ZnO. *Phys. Rev. B* **1977**, *15*, 2493−2499.
(22) Walsh, A.; Da Silva, J. L. F.; Wei, S. H. Theoretical Description of Carrier Mediated Magnetism in Cobalt Doped ZnO. *Phys. Rev. Lett.* **2008**, *100*, 256401.
(23) Lany, S.; Raebiger, H.; Zunger, A. Magnetic Interactions of Cr−Cr and Co−Co Impurity Pairs in ZnO within a Band-Gap Corrected Density Functional Approach. *Phys. Rev. B* **2008**, *77*, 241201(R).
(24) Sarsari, I. A.; Pemmaraju, C. D.; Salamati, H.; Sanvito, S. ManyBody Quasiparticle Spectrum of Co-Doped ZnO: A GW Perspective. *Phys. Rev. B* **2013**, *87*, 245118.
(25) Gopal, P.; Spaldin, N. A. Magnetic Interactions in Transition-Metal-Doped ZnO: An Ab Initio Study. *Phys. Rev. B* **2006**, *74*, 094418.
(26) Badaeva, E.; Feng, Y.; Gamelin, D. R.; Li, X. Investigation of Pure and $Co^{2+}$-Doped ZnO Quantum Dot Electronic Structures Using the Density Functional Theory: Choosing the Right Functional. *New J. Phys.* **2008**, *10*, 055013.
(27) Frisch, M. J.; Trucks, G. W.; Schlegel, H. B.; Scuseria, G. E.; Robb, M. A.; Cheeseman, J. R.; Scalmani, G.; Barone, V.; Mennucci, B.; Petersson, G. A.; et al. *Gaussian Development Version*, revision H.01; Gaussian Inc.: Wallingford, CT, 2009.
(28) Perdew, J. P.; Burke, K.; Ernzerhof, M. Generalized Gradient Approximation Made Simple. *Phys. Rev. Lett.* **1996**, *77*, 3865−3868.
(29) Perdew, J. P.; Burke, K.; Ernzerhof, M. Generalized Gradient Approximation Made Simple [Erratum]. *Phys. Rev. Lett.* **1997**, *78*, 1396.
(30) Adamo, C.; Barone, V. Toward Reliable Density Functional Methods Without Adjustable Parameters: The PBE0Model. *J. Chem. Phys.* **1999**, *110*, 6158−6170.
(31) Dunning, T. H.; Hay, P. J. In *Modern Theoretical Chemistry*; Shaefer, H. F., Ed.; Plenum: New York, 1977; Vol. 2, pp 1−28.
(32) Wadt, W. R.; Hay, P. J. Ab Initio Effective Core Potentials for Molecular Calculations — Potentials for Main Group Elements Na to Bi. *J. Chem. Phys.* **1985**, *82*, 284−298.
(33) Hay, P. J.; Wadt, W. R. Ab Initio Effective Core Potentials for Molecular Calculations — Potentials for the Transition-Metal Atoms Sc to Hg. *J. Chem. Phys.* **1985**, *82*, 270−283.
(34) Roy, L. E.; Hay, P. J.; Martin, R. L. Revised Basis Sets for the LANL Effective Core Potentials. *J. Chem. Theory Comput.* **2008**, *4*, 1029−1031.
(35) Kobayashi, M.; Ishida, Y.; Hwang, J. I.; Mizokawa, T.; Fujimori, A.; Mamiya, K.; Okamoto, J.; Takeda, Y.; Okane, T.; Saitoh, Y.; et al. Characterization of Magnetic Components in the Diluted Magnetic Semiconductor $Zn_{1-x}Co_xO$ by X-ray Magnetic Circular Dichroism. *Phys. Rev. B* **2005**, *72*, 201201(R).
(36) Wi, S. C.; Kang, J. S.; Kim, J. H.; Cho, S. B.; Kim, B. J.; Yoon, S.; Suh, B. J.; Han, S. W.; Kim, K. H.; Kim, K. J.; et al. Electronic Structure of $Zn_{1-x}Co_xO$ Using Photoemission and X-ray Absorption Spectroscopy. *Appl. Phys. Lett.* **2004**, *84*, 4233−4235.
(37) Kaspar, T. C.; Droubay, T.; Heald, S. M.; Nachimuthu, P.; Wang, C. M.; Shutthanandan, V.; Johnson, C. A.; Gamelin, D. R.; Chambers, S. A. Lack of Ferromagnetism in *N*-Type Cobalt-Doped ZnO Epitaxial Thin Films. *New J. Phys.* **2008**, *10*, 055010.
(38) Stratmann, R. E.; Scuseria, G. E.; Frisch, M. J. An Efficient Implementation of Time-Dependent Density-Functional Theory for the Calculation of Excitation Energies of Large Molecules. *J. Chem. Phys.* **1998**, *109*, 8218−8224.
(39) Badaeva, E.; May, J. W.; Ma, J.; Gamelin, D. R.; Li, X. Characterization of Excited-State Magnetic Exchange in $Mn^{2+}$-Doped ZnO Quantum Dots Using Time-Dependent Density Functional Theory. *J. Phys. Chem. C* **2011**, *115*, 20986−20991.
(40) Brus, L. E. Electron Electron and Electron-Hole Interactions in Small Semiconductor Crystallites — The Size Dependence of the Lowest Excited Electronic State. *J. Chem. Phys.* **1984**, *80*, 4403−4409.